JCTC Journal of Chemical Theory and Computation

Article

pubs.acs.org/JCTC

Comparison of Real-Time and Linear-Response Time-Dependent Density Functional Theories for Molecular Chromophores Ranging from Sparse to High Densities of States

Samat Tussupbayev,[†] Niranjan Govind,*[,‡] Kenneth Lopata,[§] and Christopher J. Cramer*[,†]

[†]Department of Chemistry, Supercomputing Institute, and Chemical Theory Center, University of Minnesota, Minneapolis, Minnesota 55455, United States

[‡]Environmental Molecular Sciences Laboratory, Pacific Northwest National Laboratory, Richland, Washington 99338, United States

[§]Department of Chemistry and Center for Computation & Technology, Louisiana State University, Baton Rouge, Louisiana 70803, United States

Supporting Information

ABSTRACT: We assess the performance of real-time time-dependent density functional theory (RT-TDDFT) for the calculation of absorption spectra of 12 organic dye molecules relevant to photovoltaics and dye-sensitized solar cells with 8 exchange-correlation functionals (3 traditional, 3 global hybrids, and 2 range-separated hybrids). We compare the calculations with traditional linear-response (LR) TDDFT and experimental spectra. In addition, we demonstrate the efficacy of the RT-TDDFT approach to calculate wide absorption spectra of two large chromophores relevant to photovoltaics and molecular switches. RT-TDDFT generally requires longer simulation times, compared to LR-TDDFT, for absorption spectra of small systems. However, it becomes more effective for the calculation of wide absorption spectra of large molecular complexes and systems with very high densities of states.

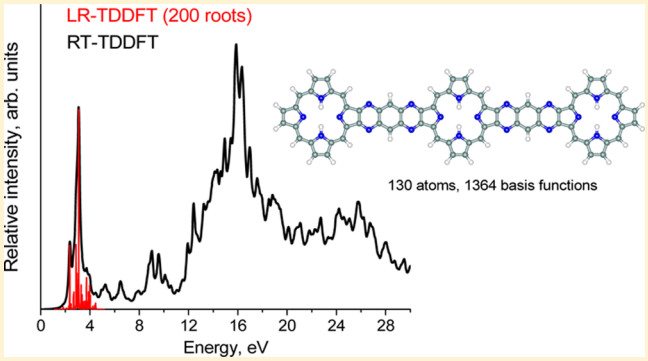

1. INTRODUCTION

The time-dependent response of molecules and materials under the influence of external fields is at the center of several fundamental processes, such as photodissociation, organic and inorganic photovoltaic systems, electron transport, charge injection, higher-order nonlinear response, etc. In a nutshell, light-matter interactions can be classified as either weak, when the interaction with the field is much smaller than the magnitude of the intermolecular interactions, and strong otherwise. In the former, the excitation is weak and results in a small perturbation away from the ground state. In this regime, perturbation theories such as linear-response or frequency domain density functional theory (LR-TDDFT) provide reliable descriptions of the linear-response properties of molecules and materials (e.g., electronic absorption spectra).[1,2] Strong interactions, on the other hand, require methodologies that go beyond linear response.

Over the past few years, there has been growing interest in real-time formulations and real-time time-dependent density functional theory (RT-TDDFT) in particular. It is an alternative approach to the traditional response formulation which allows one to capture the effects of external fields of molecules and materials in both the weak and strong interaction regimes in a seamless manner. Unlike the weak limit, where frequency domain (or linear response) perturbative approaches are sufficient, the strong limit is best captured via a real-time, real-space, and time-correlation approach. In addition to being able to simulate transient spectroscopies, where full dynamical information about the excitation process is needed, the nonlinear spectral information of molecules and materials beyond perturbation theory can also be calculated.

Due in part to its growing popularity, many implementations of RT-TDDFT have been reported in the literature[3−14] and have been used in several applications such as molecular conductance,[12,15] excited states at metal surfaces,[16] absorption properties of silicon clusters,[9] double excitations,[17] singlet−triplet transition,[18] electric circular dichroism (ECD) spectroscopy,[19] and magnetic circular dichroism (MCD) spectroscopy.[20] There has also been extensive work in developing schemes that go beyond the Born−Oppenheimer (BO) approximation to explicitly treat nuclear motion, such as Ehrenfest dynamics,[21,22] Liouville−von Neumann (LvN) molecular dynamics with real-time tight binding,[6] the use of surface hopping between adiabatic states,[23−25] and correlated electron−ion dynamics.[26] Recent implementations have also been reported in combination with solvation models,[27−29] applications to core-level spectra,[30] optical spectra of metal-

Received: August 23, 2014

DOI: 10.1021/ct500763y
J. Chem. Theory Comput. XXXX, XXX, XXX−XXX

oxides[31] and with non-Hermitian von Neumann density matrix propagation with absorbing potentials to model near and above ionization electronic excitations and core spectra.[32,63]

An important feature of RT-TDDFT is its ability to capture excitations across broad spectral regions (5−20 eV) in large systems and systems with high densities of states (DOSs). For example, the optical absorption spectrum of transition-metal oxide materials such as α-Fe_2O_3 typically involves closely spaced excitations between the O 2p and unoccupied transition-metal (Fe) 3d states.[31] Traditional methods such as LR-TDDFT may be used to address the lowest excited states. However, these "bottom-up" iterative approaches become computationally prohibitive if large numbers of excitations ($\sim 10^3-10^4$) are involved, because of the tetradic nature of the RPA matrix.[33] Formally, the numerical cost to diagonalize the full LR-TDDFT equations scales as $O(N^6)$. Similar issues are encountered in the calculation of core-level spectra (XANES).[30] RT-TDDFT, in combination with a delta-function field, addresses this by simultaneously exciting all the electronic modes with the length of the simulation determining the resolution of the spectral features. In this context, we should also mention the complex polarization,[34] damped response approaches,[35,36] and multishift linear solvers,[37] which have also been shown to be viable approaches to address wide absorption spectra. Other approaches include the self-consistent constricted variational DFT approach by Ziegler and co-workers[38] and the simplified Tamm-Dancoff[39] and simplified TDDFT reported by Grimme and co-workers.[40]

In this work, we present a systematic benchmark study, using our previously reported RT-TDDFT implementation in NWChem,[13] of the absorption spectra (or weak field limit) of 12 organic dye molecules relevant for photovoltaics and dye-sensitized solar cells using 8 exchange-correlation functionals (3 traditional, 3 global hybrids, and 2 range-separated hybrids). These calculations are compared with traditional LR-TDDFT. We also compare the RT-TDDFT calculated spectrum with the gas phase experimental spectrum for the Zn-phtalocyanine (ZnPc) system using the B3LYP and M06 functionals. Finally, to the best of our knowledge, for the first time, we calculate the wide absorption spectra of two large organic molecular complexes[41] relevant to photovoltaics and molecular switches. The primary goal of this paper is to demonstrate the consistency of the two approaches over a broad range of systems, exchange-correlation functionals and the utility of the RT-TDDFT approach for the calculation of spectra of large systems. We do not address the shortcomings of the different exchange-correlation functionals. The rest of the paper is organized as follows: we first present a brief overview of the method, followed by the computational details and a discussion of our results.

2. METHODOLOGY

In our Gaussian basis set implementation,[13] we use the single-particle reduced density matrix representation, which is given by

$$\mathbf{P}'_{\mu\nu}(t) = \sum_{i}^{N_{MO}} \mathbf{C}^{*}_{\mu i}(t)\mathbf{C}_{\nu i}(t) \tag{2}$$

where $\mathbf{C}_{\mu i}(t)$ is the time-dependent molecular orbital coefficient matrix. In the molecular orbital (MO) basis, the time evolution of the density matrix is governed by the von Neumann equation:

$$i\frac{\partial \mathbf{P}'(t)}{\partial t} = [\mathbf{F}'(t), \mathbf{P}'(t)] \tag{3}$$

where $\mathbf{F}'(t)$ is the time-dependent Fock matrix, which also includes the applied field, in the MO basis. For every time step, $\mathbf{P}'$ is propagated forward in time using the second-order Magnus scheme.[13]

For convenience, relative intensities are typically computed directly from the Fourier transform of the dipole moment; however, in principle, RT-TDDFT spectra yield meaningful absolute values of the oscillator strengths identical to those of LR-TDDFT. First, the on-diagonals of the complex polarizability tensor are computed from *x*,*y*,*z* kick-type excitation simulations:

$$\alpha_{ii}(\omega) = \frac{\mu_i(\omega)}{E_i(\omega)} \qquad i = x, y, z \tag{4}$$

where $\mu_i(\omega)$ and $E_i(\omega)$ are the Fourier transforms of the dipole moment and applied electric fields in the *i* direction (the off-diagonals are assumed to be zero). The absorption cross section tensor is then given by

$$\boldsymbol{\sigma}(\omega) = \frac{4\pi\omega}{c}\,\mathrm{Im}[\boldsymbol{\alpha}(\omega)] \tag{5}$$

and the resulting dipole strength function is then

$$S(\omega) = \frac{1}{3}\,\mathrm{Tr}[\boldsymbol{\sigma}(\omega)] \tag{6}$$

It is worth emphasizing that the RT-TDDFT approach is dependent only on the exchange-correlation potential via the time-dependent Fock matrix, unlike the LR-TDDFT approach, which requires the full second derivative of the exchange-correlation functional as part of the response equations. This not only simplifies the implementation, but also removes the dependence on higher derivatives and potential numerical instabilities that may stem from them. As such, this approach can also be used to test the accuracy of response properties and excited states from potential-driven density functional theory, i.e., for exchange-correlation functionals which have no energy functional or for which higher derivatives have not yet been implemented. For further details of the implementation and information about time propagators, we refer the interested reader to our original paper.[13]

Computational Details. All calculations were performed with the NWChem 6.3 software suite,[42] except for linear-response (LR-TDDFT) calculations employing meta-GGA functionals, which were done using the Gaussian 09 software suite.[43] In total, eight exchange-correlation functionals were considered and were divided into three groups, depending on the amount of HF exchange. Three local functionals were considered (BLYP,[44,45] M06-L,[46] and M11-L[47] (which has dual-range DFT exchange)), along with three global hybrids (B3LYP (VWN5 version),[45,48−50] M06, and M06-2X,[51] with 20%, 27%, and 54% Hartree−Fock (HF) exchange, respectively), and two range-separated hybrids (CAM-B3LYP[52] and M11,[53] with 19% and 42.8% HF exchange, respectively, in the short range and 65% and 100% HF exchange, respectively, in the long range).

The dyes considered in this study vary in size from 14 atoms for the smallest (2,3,5-trifluorobenzaldehyde) to 162 atoms for the largest (*f*-coronene) and cover both organic and organometallic compounds. They include 2,3,5-trifluorobenzaldehyde (**1**), dibenzonaphthyridindione (**2**), coronene (**3**), coumarin

DOI: 10.1021/ct500763y
J. Chem. Theory Comput. XXXX, XXX, XXX−XXX

153 (**4**), 4′-hydroxybenzylidene-2,3-dimethylimidazoline (**5**), indigo (**6**), naphthacene (**7**), oligoporphyrin dimer (P2TA, **8**), phthalocyanine (**9**), zinc phthalocyanine (**10**), 3′,4′-dibutyl-2-phenyl-2,2′:5′,2″-terthiophene-5″-carboxylic acid (**11**), *cis*-[Ru-(4,4′-COOH-2,2′-bpy)$_2$(NCS)$_2$] complex (also known as N3, **12**), P3B2 ($C_{72}H_{38}N_{20}$, **13**), and *f*-coronene ($C_{108}H_{42}N_{12}$, **14**). The ground-state geometries of molecules **1**−**10**, as well as **13** and **14**, were optimized at the B3LYP/6-31G(d) level,[54,55] while molecules **11** and **12** were optimized using BHLYP-D3/def2-SVP[45,56−58] and B3LYP/def2-SVP[59] methods, respectively. BHLYP was employed for geometry optimization of molecule **11**, in order to correctly reproduce the experimental absorption spectrum peak at 3.30 eV.[60] The BHLYP functional with 50% HF exchange was used, since Adamo and coworkers[61] previously showed that, for long-chain conjugated systems, only functionals with high Hartree−Fock contribution (global hybrid or long-range corrected) correctly reproduce bond length alternation. The structures are shown in Figure 1, and the coordinates are provided as part of the Supporting Information.

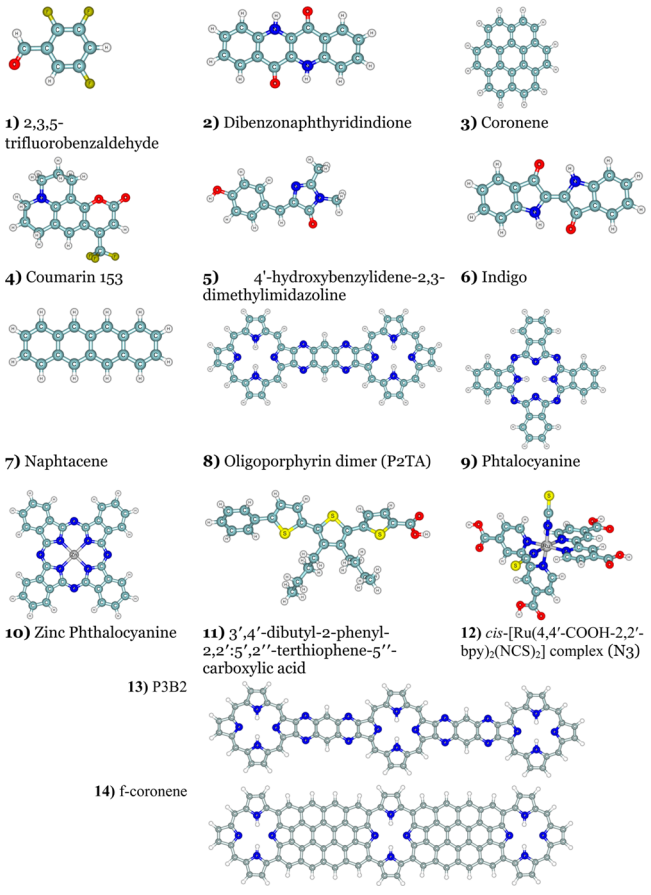

Figure 1. Benchmark chromophores used in this work.

All LR- and RT-TDDFT calculations were performed with the 6-31G(d) basis,[54,55] except for molecules **11** and **12**, which were calculated with the def2-SVP basis[57,58] and def2-ECP for Ru.[59] While these basis sets are smaller than would generally be chosen for highly accurate calculations, it is convenient here, where our goal is, instead, to compare methodologies against each other for a large number of excitations. Forty (40) LR excited states were calculated for all molecules, except for the P3B2 system (molecule **13**), where 200 excitations were calculated. The ground-state single-point DFT calculations to generate the initial density for RT-TDDFT were run with a tighter density convergence (RMS difference of $<10^{-9}$) to avoid numerical error accumulation. The default convergence criteria (RMS difference of 10^{-5}) led to artifacts in the absorption spectra for some of the dye molecules; therefore, tighter density convergence criteria are recommended. The real-time calculations were carried out with a time step Δt = 0.2 a.u. = 0.0048 fs and propagated for 5000 time steps, which corresponds to 24.2 fs (or 1000 a.u.). To resolve an excitation of energy ω, the time step must be smaller than π/ω, and the accuracy is typically a tenth of that. An electric field pulse in the form of a small δ-kick with field strength $\kappa = 2 \times 10^{-5}$ a.u. = 10 mV/nm was used to simultaneously excite all electronic modes. To accelerate the convergence of the Fourier transform, the time signals were damped by $e^{-t/\tau}$ (where τ = 200 a.u. = 6 fs), which yielded artificially Lorentzian broadened peaks in the absorption spectra. For core-level spectra, smaller time steps (∼0.02−0.005 au) are needed, as shown in ref 28.

3. RESULTS AND DISCUSSION

As one benchmark measure, for each chromophore, we chose the most intense feature in the spectrum in the energy range (2−8 eV) from standard LR-TDDFT calculations to compare with RT-TDDFT. This typically, but not always, corresponded to the highest occupied molecular orbital−lowest unoccupied molecular orbital (HOMO−LUMO) transition for the systems considered. The absorption energies of these peaks are summarized in Table 1. As expected, for most dyes, the excitation energies increase with the amount of HF exchange in the exchange-correlation functional. Local functionals based on the Minnesota family, M06-L and M11-L, yield energies that lie between those of BLYP and B3LYP. M06 gives slightly higher excitation energies, compared with B3LYP, and M11 yields higher energies, compared with CAM-B3LYP. Exceptions to this trend are observed in phthalocyanine and zinc phthalocyanine (molecules **9** and **10**), which are insensitive to the nature of the density functional used.

Overall, the vertical singlet excitation energies calculated with LR-TDDFT and RT-TDDFT are in excellent agreement with each other, with the largest deviation being ∼0.07 eV (∼2%) for dye molecules **2** and **4**, computed with M11. Mean unsigned deviation (MUD) values between the two methodologies over all dyes are also reported in Table 1, and these range from 0.007 eV to 0.02 eV. These deviations are due to signal processing errors, since, in principle, LR-TDDFT and RT-TDDFT are equivalent in the weak-field regime. In Figure 2 and Table 2, we compare the RT-TDDFT calculated spectrum with experimental results for the ZnPc system, using the B3LYP and M06 functionals and 6-31G(d) basis. The results are in good agreement over a broad range of 1.5−8.5 eV.

Even though RT-TDDFT requires long simulation times compared with LR-TDDFT for the calculation of absorption spectra in small systems, it becomes more effective for the calculation of wide absorption spectra of large complexes and systems with very high DOSs. Here, we demonstrate this by calculating the absorption spectra of two large organic molecules, namely, P3B2 and f-coronene (molecules **13** and **14** in Figure 1). P3B2 and *f*-coronene are comprised of 130 and 162 atoms, and require 1364 and 1764 basis functions with the 6-31G(d) basis set, respectively. In Figure 5, we plot the convergence of the absorption spectrum with respect to the total simulation times for the P3B2 molecule.

DOI: 10.1021/ct500763y
J. Chem. Theory Comput. XXXX, XXX, XXX−XXX

Table 1. Calculated Gas-Phase Vertical Singlet Excitation Energies for the Dye Benchmark Set

	Excitation Energy[a] (eV)							
	BLYP[a]	B3LYP	CAM-B3LYP	M06-L	M06	M06-2X	M11-L	M11
1	**3.75**	**4.31**	**4.69**	**4.04**	**4.40**	**4.83**	**4.15**	**4.88**
	3.73	4.30	4.69	4.03	4.38	4.81	4.15	4.87
2	**2.70**	**3.11**	**3.55**	**2.89**	**3.23**	**3.53**	**2.86**	**3.74**
	2.69	3.10	3.53	2.89	3.22	3.52	2.86	3.67
3	**3.75**	**4.15**	**4.66**	**3.95**	**4.20**	**4.63**	**3.87**	**4.91**
	3.74	4.15	4.65	3.94	4.19	4.63	3.87	4.91
4	**2.95**	**3.36**	**3.78**	**3.16**	**3.43**	**3.76**	**3.11**	**3.98**
	2.94	3.36	3.76	3.15	3.44	3.76	3.13	3.91
5	**3.25**	**3.54**	**3.79**	**3.47**	**3.57**	**3.78**	**3.42**	**3.87**
	3.25	3.54	3.79	3.46	3.58	3.78	3.42	3.86
6	**2.04**	**2.32**	**2.61**	**2.21**	**2.41**	**2.58**	**2.18**	**2.66**
	2.04	2.30	2.59	2.20	2.40	2.57	2.18	2.64
7	**2.21**	**2.49**	**2.84**	**2.32**	**2.50**	**2.86**	**2.24**	**3.06**
	2.20	2.49	2.85	2.32	2.49	2.86	2.23	3.06
8	**2.07**	**2.41**	**3.06**	**2.16**	**2.46**	**3.02**	**2.13**	**3.28**
	2.05	2.40	3.04	2.17	2.44	3.00	2.15	3.28
9	**1.99**	**2.08**	**2.07**	**2.05**	**2.02**	**2.11**	**1.99**	**1.98**
	1.99	2.09	2.05	2.06	2.02	2.12	1.99	2.00
10	**1.99**	**2.10**	**2.06**	**2.07**	**2.02**	**2.11**	**1.99**	**1.99**
	1.99	2.09	2.04	2.06	2.02	2.11	1.99	1.98
11	**2.75**	**3.23**	**3.70**	**2.94**	**3.31**	**3.72**	**2.78**	**3.93**
	2.74	3.22	3.70	2.93	3.31	3.71	2.88	3.94
12	**1.55**	**1.76**		**1.69**	**1.90**	**1.96**	**1.52**	
	1.55	1.77		1.65	1.91	1.96	1.54	
MUD[b]	0.009	0.007	0.015	0.010	0.010	0.007	0.015	0.020

[a]Values shown in boldface font represent RT-TDDFT results; values shown in normal font represent LR-TDDFT results. [b]Mean unsigned deviation over available data; the average of the LR-TDDFT roots for **10** are chosen; the higher-energy LR-TDDFT root for **8** is chosen for M11-L and M11.

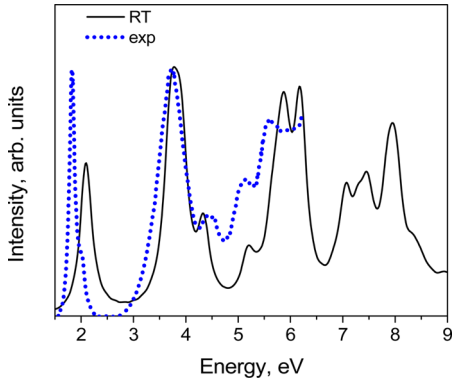

Figure 2. Real-time time-dependent density functional theory (RT-TDDFT) and gas-phase experimental[64] spectra of the ZnPc (molecule **10**) system. The RT-TDDFT spectrum was calculated at the B3LYP/6-31G(d) theory level.

Table 2. Calculated Excitation Energies (E) and Oscillator Strengths (f) Compared with Experimental Data

RT-TDDFT				
(B3LYP/6-31G(d))		(M06/6-31G(d))		Exp[a]
E (eV)	f	E (eV)	f	E (eV)
2.10	0.66	2.01	0.50	1.88
3.78	1.10	3.84	0.86	3.80
4.32	0.45	4.41	0.31	4.49
5.21	0.31	5.18	0.17	5.17
5.88, 6.17	0.97, 1.00	5.94	1.00	5.63
7.07, 7.45	0.59, 0.62	7.32	0.58	6.89
7.94	0.83	8.02	0.44	7.75

[a]Data for ZnPc in gas-phase, from ref 64.

The broad spectra, shown in Figures 3 and 4, are approximately equivalent to several thousand excitations, which is computationally prohibitive within the traditional

DOI: 10.1021/ct500763y
J. Chem. Theory Comput. XXXX, XXX, XXX−XXX

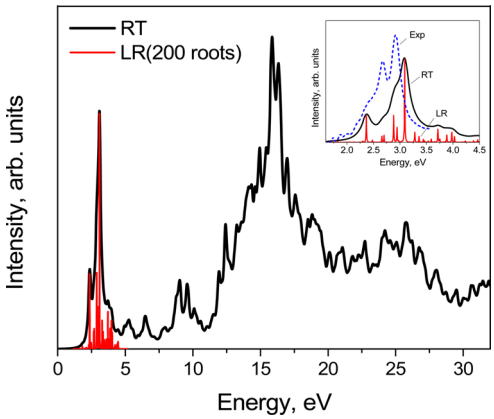

Figure 3. Linear-response (LR) and real-time (RT) TDDFT absorption spectra of P3B2 (**13**), calculated using the B3LYP functional in combination with the 6-31G(d) basis set. Inset shows a fragment of the calculated absorption spectra of P3B2, along with the experimental spectrum from refs 65 and 66.

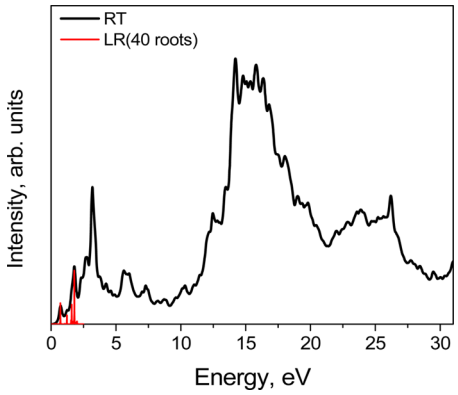

Figure 4. Linear-response (LR) and real-time (RT) TDDFT absorption spectra of *f*-coronene (**14**), calculated using the B3LYP functional in combination with the 6-31G(d) basis set.

linear-response approach. Therefore, with LR-TDDFT, we have only calculated the first 200 and 40 excitations for these two molecules, respectively. The computational efficiency of the two methods can be illustrated as follows. For the P3B2 absorption spectrum (Figure 3), RT-TDDFT calculations were run for a total simulation time of 1000 a.u. for 32 h on 1376 cores for each direction (x, y, and z)—a total time of 96 h. On the other hand, the LR-TDDFT calculation (200 excitations) was run for 13 h on the same number of cores. This suggests that RT-TDDFT calculations are roughly a factor of 7 slower, compared with LR-TDDFT. However, as we can see from Figure 5, a total simulation time of 600 a.u. is already sufficient in that the essential features are captured, albeit artificially broadened. This suggests that RT-TDDFT is only ∼4.0 times slower, compared with LR-TDDFT, but with a much wider spectral range. Unfortunately, strictly speaking, it is not possible to compare the exact number of states calculated with the two approaches, because the RT-TDDFT spectrum, assuming a sufficiently long simulation time, contains all states with nonzero oscillator strength while LR-TDDFT contains both bright and dark transitions but over a smaller spectral range. However, approximately speaking, we estimate RT-TDDFT to be roughly as fast as LR-TDDFT over a small spectral range for large systems. However, as we have emphasized, our target is

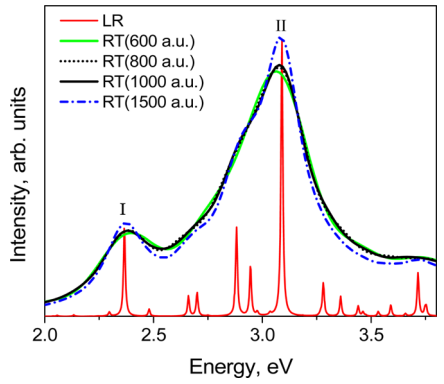

Figure 5. Convergence of RT-TDDFT, with respect to the total simulation times (600, 800, 1000, and 1500 a.u.) for the P3B2 system (molecule **13**). For clarity, we only plot a fragment of the linear response (LR) and real-time (RT) absorption spectra. [Peak I: LR, 2.36 eV; RT, 2.40 eV (600 a.u.), 2.39 eV (800 a.u.), 2.38 eV (1000 a.u.), 2.38 eV (1500 a.u.). Peak II: LR, 3.09 eV; RT, 3.06 eV (600 a.u.), 3.07 eV (800 a.u.), 3.08 eV (1000 a.u.), 3.08 eV (1500 a.u.).]

the calculation of absorption spectra over a broad range in large systems.

Overall, good agreement is observed between the two approaches for corresponding stand-alone peaks in the lower-energy range of the spectra. We are not aware of any experimental spectra for these systems with the same energy range against which to compare our calculated spectra. The only spectrum that was found in the literature is the one of P3B2 in a narrow energy range: 1.5−3.5 eV (Figure 3, inset), which agrees well with the calculated ones. It is also important to note that these energy ranges are above-ionization and, other than resonance states, unlikely to have experimentally observable absorption features. In addition, the calculated above-ionization excited states are also likely to be inaccurate because of spurious high-energy finite basis artifacts.[31] In a nutshell, these proof-of-principle calculations (recall Figures 3 and 4) are meant to highlight the utility of the approach for the calculation of large numbers of excited states and systems with large DOSs.

Since RT-TDDFT is a time-domain technique, it does not provide insight into the orbital content of the excitations as in traditional LR-TDDFT calculations. This information, in principle, is available in the time-dependent density matrix but nontrivial to extract. A possible approach is to relate the transition density at a specific frequency to the imaginary part of the Fourier transform of the time-dependent density fluctuations, with respect to the ground-state density.[62] As we have not yet implemented this in our code, we interpret features by comparing to LR-TDDFT calculations restricted to excitation windows covering regions of interest.

4. SIGNIFICANCE AND CONCLUSIONS

This systematic benchmark study demonstrates the consistency of the LR and RT approaches for absorption spectra in the weak field limit and highlights the versatility of the RT-TDDFT approach for the calculation of wide absorption spectra in large molecular complexes where the LR approach becomes impractical because of the very large number of excitations that must be considered. Therefore, we expect the RT approach to be particularly useful for optical properties of transition-metal oxides with very high DOS and dyes bound to solid interfaces, where irrespective of the density of excited electronic

DOI: 10.1021/ct500763y
J. Chem. Theory Comput. XXXX, XXX, XXX−XXX

states of the dye, there are likely to be large numbers of excited states that involve charge transfer from the dye to the solid (or vice versa). Moreover, RT-TDDFT is an excellent tool for evaluating newly developed functionals for their excited-state response, since it is dependent only on the exchange-correlation potential and does not require higher derivatives of the exchange-correlation functional, which can be cumbersome to implement in some cases.

■ ASSOCIATED CONTENT

Supporting Information

Additional data from the systems we have investigated but not included in this paper. This material is available free of charge via the Internet at http://pubs.acs.org/.

■ AUTHOR INFORMATION

Corresponding Authors

*E-mail: niri.govind@pnnl.gov (N. Govind).
*E-mail: cramer@umn.edu (C. J. Cramer).

Notes

The authors declare no competing financial interest.

■ ACKNOWLEDGMENTS

This material is based upon work supported by the U.S. Department of Energy, Office of Science, Office of Advanced Scientific Computing Research, Scientific Discovery through Advanced Computing (SciDAC) program, under Award No. DE-SC0008666. This research used resources of the National Energy Research Scientific Computing Center, a DOE Office of Science User Facility supported by the Office of Science of the U.S. Department of Energy, under Contract No. DE-AC02-05CH11231. K.L. gratefully acknowledges support from the LSU Office of Research and Development, as well as the Louisiana Board of Regents Research Competitiveness Subprogram, under Contract No. LEQSF(2014-17)-RD-A-03. N.G. thanks Jeffrey Reimers for useful discussions regarding the P3B2 and f-coronene molecular systems. A portion of the research was performed using EMSL, a DOE Office of Science User Facility sponsored by the Office of Biological and Environmental Research and located at Pacific Northwest National Laboratory.

■ REFERENCES

(1) Marques, M. A. L.; Ullrich, C. A.; Nogueira, F.; Rubio, A.; Burke, K.; Gross, E. K. U. Time-Dependent Density Functional Theory. In *Lecture Notes in Physics*, Vol. *706*; Springer: New York, 2006; p 555.

(2) Casida, M. E.; Huix-Rotllant, M. Progress in Time-Dependent Density-Functional Theory. *Annu. Rev. Phys. Chem.* **2012**, *63*, 287−323.

(3) Theilhaber, J. Abinitio Simulations of Sodium Using Time-Dependent Density-Functional Theory. *Phys. Rev. B* **1992**, *46*, 12990−13003.

(4) Yabana, K.; Bertsch, G. F. Time-dependent local-density approximation in real time. *Phys. Rev. B* **1996**, *54*, 4484−4487.

(5) Castro, A.; Appel, H.; Oliveira, M.; Rozzi, C. A.; Andrade, X.; Lorenzen, F.; Marques, M. A. L.; Gross, E. K. U.; Rubio, A. Octopus: A tool for the application of time-dependent density functional theory. *Phys. Status Solidi B* **2006**, *243*, 2465−2488.

(6) Jakowski, J.; Morokuma, K. Liouville−von Neumann molecular dynamics. *J. Chem. Phys.* **2009**, *130*.

(7) Li, X. S.; Smith, S. M.; Markevitch, A. N.; Romanov, D. A.; Levis, R. J.; Schlegel, H. B. A time-dependent Hartree−Fock approach for studying the electronic optical response of molecules in intense fields. *Phys. Chem. Chem. Phys.* **2005**, *7*, 233−239.

(8) Takimoto, Y.; Vila, F. D.; Rehr, J. J. Real-time time-dependent density functional theory approach for frequency-dependent nonlinear optical response in photonic molecules. *J. Chem. Phys.* **2007**, *127*.

(9) Sun, J.; Song, J.; Zhao, Y.; Liang, W. Z. Real-time propagation of the reduced one-electron density matrix in atom-centered Gaussian orbitals: Application to absorption spectra of silicon clusters. *J. Chem. Phys.* **2007**, *127*.

(10) Meng, S.; Kaxiras, E. Real-time, local basis-set implementation of time-dependent density functional theory for excited state dynamics simulations. *J. Chem. Phys.* **2008**, *129*.

(11) Baer, R.; Neuhauser, D. Real-time linear response for time-dependent density-functional theory. *J. Chem. Phys.* **2004**, *121*, 9803−9807.

(12) Cheng, C. L.; Evans, J. S.; Van Voorhis, T. Simulating molecular conductance using real-time density functional theory. *Phys. Rev. B* **2006**, *74*.

(13) Lopata, K.; Govind, N. Modeling Fast Electron Dynamics with Real-Time Time-Dependent Density Functional Theory: Application to Small Molecules and Chromophores. *J. Chem. Theory Comput.* **2011**, *7*, 1344−1355.

(14) Gao, B.; Ruud, K.; Luo, Y. Plasmon resonances in linear noble-metal chains. *J. Chem. Phys.* **2012**, *137*.

(15) Evans, J. S.; Van Voorhis, T. Dynamic Current Suppression and Gate Voltage Response in Metal−Molecule−Metal Junctions. *Nano Lett.* **2009**, *9*, 2671−2675.

(16) Li, X. S.; Tully, J. C. Ab initio time-resolved density functional theory for lifetimes of excited adsorbate states at metal surfaces. *Chem. Phys. Lett.* **2007**, *439*, 199−203.

(17) Isborn, C. M.; Li, X. S. Modeling the doubly excited state with time-dependent Hartree-Fock and density functional theories. *J. Chem. Phys.* **2008**, *129*.

(18) Isborn, C. M.; Li, X. S. Singlet−Triplet Transitions in Real-Time Time-Dependent Hartree-Fock/Density Functional Theory. *J. Chem. Theory Comput.* **2009**, *5*, 2415−2419.

(19) Yabana, K.; Bertsch, G. F. Application of the time-dependent local density approximation to optical activity. *Phys. Rev. A* **1999**, *60*, 1271−1279.

(20) Lee, K. M.; Yabana, K.; Bertsch, G. F. Magnetic circular dichroism in real-time time-dependent density functional theory. *J. Chem. Phys.* **2011**, 134.

(21) Li, X. S.; Tully, J. C.; Schlegel, H. B.; Frisch, M. J. Ab initio Ehrenfest dynamics. *J. Chem. Phys.* **2005**, 123.

(22) Livshits, E.; Baer, R. Time-dependent density-functional studies of the D-2 Coulomb explosion. *J. Phys. Chem. A* **2006**, *110*, 8443−8450.

(23) Craig, C. F.; Duncan, W. R.; Prezhdo, O. V. Trajectory surface hopping in the time-dependent Kohn−Sham approach for electron-nuclear dynamics. *Phys. Rev. Lett.* **2005**, 95.

(24) Duncan, W. R.; Stier, W. M.; Prezhdo, O. V. Ab initio nonadiabatic molecular dynamics of the ultrafast electron injection across the alizarin−TiO_2 interface. *J. Am. Chem. Soc.* **2005**, *127*, 7941−7951.

(25) Zhang, X.; Li, Z.; Lu, G. First-principles determination of charge carrier mobility in disordered semiconducting polymers. *Phys. Rev. B* **2010**, 82.

(26) Stella, L.; Meister, M.; Fisher, A. J.; Horsfield, A. P. Robust nonadiabatic molecular dynamics for metals and insulators. *J. Chem. Phys.* **2007**, 127.

(27) Liang, W.; Chapman, C. T.; Ding, F. Z.; Li, X. S. Modeling Ultrafast Solvated Electronic Dynamics Using Time-Dependent Density Functional Theory and Polarizable Continuum Model. *J. Phys. Chem. A* **2012**, *116*, 1884−1890.

(28) Nguyen, P. D.; Ding, F. Z.; Fischer, S. A.; Liang, W. K.; Li, X. S. Solvated First-Principles Excited-State Charge-Transfer Dynamics with Time-Dependent Polarizable Continuum Model and Solvent Dielectric Relaxation. *J. Phys. Chem. Lett.* **2012**, *3*, 2898−2904.

(29) Pipolo, S.; Corni, S.; Cammi, R. The cavity electromagnetic field within the polarizable continuum model of solvation: An application to

DOI: 10.1021/ct500763y
J. Chem. Theory Comput. XXXX, XXX, XXX−XXX

the real-time time dependent density functional theory. *Comput. Theor. Chem.* **2014**, *1040*−*1041*, 112−119.
(30) Lopata, K.; Van Kuiken, B. E.; Khalil, M.; Govind, N. Linear-Response and Real-Time Time-Dependent Density Functional Theory Studies of Core-Level Near-Edge X-Ray Absorption. *J. Chem. Theory Comput.* **2012**, *8*, 3284−3292.
(31) Wang, Y.; Lopata, K.; Chambers, S. A.; Govind, N.; Sushko, P. V. Optical Absorption and Band Gap Reduction in $(Fe_{1-x}Cr_x)_2O_3$ Solid Solutions: A First-Principles Study. *J. Phys. Chem. C* **2013**, *117*, 25504−25512.
(32) Lopata, K.; Govind, N. Near and Above Ionization Electronic Excitations with Non-Hermitian Real-Time Time-Dependent Density Functional Theory. *J. Chem. Theory Comput.* **2013**, *9*, 4939−4946.
(33) Tretiak, S.; Isborn, C. M.; Niklasson, A. M. N.; Challacombe, M. Representation independent algorithms for molecular response calculations in time-dependent self-consistent field theories. *J. Chem. Phys.* **2009**, 130.
(34) (a) Kauczor, J.; Norman, P. Efficient Calculations of Molecular Linear Response Properties for Spectral Regions. *J. Chem. Theory Comput.* **2014**, *10*, 2449−2455. (b) Norman, P.; Bishop, D. M.; Jensen, H. J. A.; Oddershede, J. Near-resonant absorption in the time-dependent self-consistent field and multiconfigurational self-consistent field approximations. *J. Chem. Phys.* **2001**, *115*, 10323−10334. (c) Norman, P.; Bishop, D. M.; Jensen, H. J. A.; Oddershede, J. Nonlinear response theory with relaxation: The first-order hyperpolarizability. *J. Chem. Phys.* **2005**, 123.
(35) Jensen, L.; Autschbach, J.; Schatz, G. C. Finite lifetime effects on the polarizability within time-dependent density-functional theory. *J. Chem. Phys.* **2005**, 122.
(36) Devarajan, A.; Gaenko, A.; Autschbach, J. Two-component relativistic density functional method for computing nonsingular complex linear response of molecules based on the zeroth order regular approximation. *J. Chem. Phys.* **2009**, 130.
(37) Hübener, H.; Giustino, F. Linear optical response of finite systems using multishift linear system solvers. *J. Chem. Phys.* **2014**, 141.
(38) Ziegler, T.; Krykunov, M.; Cullen, J. The implementation of a self-consistent constricted variational density functional theory for the description of excited states. *J. Chem. Phys.* **2012**, *136*.
(39) Grimme, S. A simplified Tamm−Dancoff density functional approach for the electronic excitation spectra of very large molecules. *J. Chem. Phys.* **2013**, 138.
(40) Bannwarth, C.; Grimme, S. A simplified time-dependent density functional theory approach for electronic ultraviolet and circular dichroism spectra of very large molecules. *Comput. Theor. Chem.* **2014**, *1040*, 45−53.
(41) Reimers, J. R.; Hall, L. E.; Crossley, M. J.; Hush, N. S. Rigid fused oligoporphyrins as potential versatile molecular wires. 2. B3LYP and SCF calculated geometric and electronic properties of 98 oligoporphyrin and related molecules. *J. Phys. Chem. A* **1999**, *103*, 4385−4397.
(42) Valiev, M.; Bylaska, E. J.; Govind, N.; Kowalski, K.; Straatsma, T. P.; Van Dam, H. J. J.; Wang, D.; Nieplocha, J.; Apra, E.; Windus, T. L.; de Jong, W. NWChem: A comprehensive and scalable open-source solution for large scale molecular simulations. *Comput. Phys. Commun.* **2010**, *181*, 1477−1489.
(43) Frisch, M. J.; Trucks, G. W.; Schlegel, H. B.; Scuseria, G. E.; Robb, M. A.; Cheeseman, J. R.; Scalmani, G.; Barone, V.; Mennucci, B.; Petersson, G. A.; Nakatsuji, H.; Caricato, M.; Li, X.; Hratchian, H. P.; Izmaylov, A. F.; Bloino, J.; Zheng, G.; Sonnenberg, J. L.; Hada, M.; Ehara, M.; Toyota, K.; Fukuda, R.; Hasegawa, J.; Ishida, M.; Nakajima, T.; Honda, Y.; Kitao, O.; Nakai, H.; Vreven, T.; Montgomery, J. A., Jr.; Peralta, J. E.; Ogliaro, F.; Bearpark, M.; Heyd, J. J.; Brothers, E.; Kudin, K. N.; Staroverov, V. N.; Kobayashi, R.; Normand, J.; Raghavachari, K.; Rendell, A.; Burant, J. C.; Iyengar, S. S.; Tomasi, J.; Cossi, M.; Rega, N.; Millam, J. M.; Klene, M.; Knox, J. E.; Cross, J. B.; Bakken, V.; Adamo, C.; Jaramillo, J.; Gomperts, R.; Stratmann, R. E.; Yazyev, O.; Austin, A. J.; Cammi, R.; Pomelli, C.; Ochterski, J. W.; Martin, R. L.; Morokuma, K.; Zakrzewski, V. G.; Voth, G. A.; Salvador, P.; Dannenberg, J. J.; Dapprich, S.; Daniels, A. D.; Farkas, Ö.; Foresman, J. B.; Ortiz, J. V.; Cioslowski, J.; Fox, D. J. *Gaussian 09*, Revision D.01; Gaussian, Inc.: Wallingford, CT, 2009.
(44) Becke, A. D. Density-Functional Exchange-Energy Approximation with Correct Asymptotic-Behavior. *Phys. Rev. A* **1988**, *38*, 3098−3100.
(45) Lee, C. T.; Yang, W. T.; Parr, R. G. Development of the Colle−Salvetti Correlation-Energy Formula into a Functional of the Electron-Density. *Phys. Rev. B* **1988**, *37*, 785−789.
(46) Zhao, Y.; Truhlar, D. G. A new local density functional for main-group thermochemistry, transition metal bonding, thermochemical kinetics, and noncovalent interactions. *J. Chem. Phys.* **2006**, *125*.
(47) Peverati, R.; Truhlar, D. G. M11-L: A Local Density Functional That Provides Improved Accuracy for Electronic Structure Calculations in Chemistry and Physics. *J. Phys. Chem. Lett.* **2012**, *3*, 117−124.
(48) Becke, A. D. Density-Functional Thermochemistry. 3. The Role of Exact Exchange. *J. Chem. Phys.* **1993**, *98*, 5648−5652.
(49) Vosko, S. H.; Wilk, L.; Nusair, M. Accurate Spin-Dependent Electron Liquid Correlation Energies for Local Spin-Density Calculations—A Critical Analysis. *Can. J. Phys.* **1980**, *58*, 1200−1211.
(50) Stephens, P. J.; Devlin, F. J.; Chabalowski, C. F.; Frisch, M. J. Ab-Initio Calculation of Vibrational Absorption and Circular-Dichroism Spectra Using Density-Functional Force-Fields. *J. Phys. Chem.* **1994**, *98*, 11623−11627.
(51) Zhao, Y.; Truhlar, D. G. The M06 suite of density functionals for main group thermochemistry, thermochemical kinetics, noncovalent interactions, excited states, and transition elements: Two new functionals and systematic testing of four M06-class functionals and 12 other functionals. *Theor. Chem. Acc.* **2008**, *120*, 215−241.
(52) Yanai, T.; Tew, D. P.; Handy, N. C. A new hybrid exchange-correlation functional using the Coulomb-attenuating method (CAM-B3LYP). *Chem. Phys. Lett.* **2004**, *393*, 51−57.
(53) Peverati, R.; Truhlar, D. G. Improving the Accuracy of Hybrid Meta-GGA Density Functionals by Range Separation. *J. Phys. Chem. Lett.* **2011**, *2*, 2810−2817.
(54) Hehre, W. J.; D, R.; Pople, J. A. Self-Consistent Molecular Orbital Methods. XII. Further Extensions of Gaussian-Type Basis Sets for Use in Molecular Orbital Studies of Organic Molecules. *J. Chem. Phys.* **1972**, *56*, 2257−2261.
(55) Hariharan, P. C.; Pople, J. A. The influence of polarization functions on molecular orbital hydrogenation energies. *Theor. Chim. Acta* **1973**, *28*, 213−222.
(56) Becke, A. D. A New Mixing of Hartree−Fock and Local Density-Functional Theories. *J. Chem. Phys.* **1993**, *98*, 1372−1377.
(57) Grimme, S.; Antony, J.; Ehrlich, S.; Krieg, H. A consistent and accurate ab initio parametrization of density functional dispersion correction (DFT-D) for the 94 elements H-Pu. *J. Chem. Phys.* **2010**, 132.
(58) Weigend, F.; Ahlrichs, R. Balanced basis sets of split valence, triple zeta valence and quadruple zeta valence quality for H to Rn: Design and assessment of accuracy. *Phys. Chem. Chem. Phys.* **2005**, *7*, 3297−3305.
(59) Andrae, D.; Haussermann, U.; Dolg, M.; Stoll, H.; Preuss, H. Energy-Adjusted Abinitio Pseudopotentials for the 2nd and 3rd Row Transition-Elements. *Theor. Chim. Acta* **1990**, *77*, 123−141.
(60) Huss, A. S.; Rossini, J. E.; Ceckanowicz, D. J.; Bohnsack, J. N.; Mann, K. R.; Gladfelter, W. L.; Blank, D. A. Photoinitiated Electron Transfer Dynamics of a Terthiophene Carboxylate on Monodispersed Zinc Oxide Nanocrystals. *J. Phys. Chem. C* **2011**, *115*, 2−10.
(61) Jacquemin, D.; Adamo, C. Bond Length Alternation of Conjugated Oligomers: Wave Function and DFT Benchmarks. *J. Chem. Theory Comput.* **2011**, *7*, 369−376.
(62) Hofmann, D.; Kummel, S. Self-interaction correction in a real-time Kohn−-Sham scheme: Access to difficult excitations in time-dependent density functional theory. *J. Chem. Phys.* **2012**, *137*.
(63) Fernando, R. G.; Balhoff, M. C.; Lopata, K. X-ray Absorption in Insulators with Non-Hermitian Real-Time Time-Dependent Density Functional Theory. **2014**, *J. Chem. Theory Comput.* DOI: 10.1021/ct500943m.

DOI: 10.1021/ct500763y
J. Chem. Theory Comput. XXXX, XXX, XXX−XXX

(64) Edwards, L.; Gouterman, M. Porphyrins XV. Vapor Absorption Spectra and Stability: Phthalocyanines. *J. Mol. Spectrosc.* **1970**, *33*, 292.
(65) Maynard, P. J. *Oligomeric planar porphyrins*; Ph.D. Dissertation, University of Sydney, Sydney, NSW, Australia, 1992.
(66) Hough, W. A. *Synthesis and properties of oligoporphyrins*; Ph.D. Dissertation, University of Sydney, Sydney, NSW, Australia, 2003.

DOI: 10.1021/ct500763y
J. Chem. Theory Comput. XXXX, XXX, XXX−XXX